Cite this: *Faraday Discuss.*, 2013, **164**, 189

Electrochemical mechanical micromachining based on confined etchant layer technique

Ye Yuan,[a] Lianhuan Han,[a] Jie Zhang,[a] Jingchun Jia,[a] Xuesen Zhao,[b] Yongzhi Cao,[b] Zhenjiang Hu,*[b] Yongda Yan,[b] Shen Dong,[b] Zhong-Qun Tian,[a] Zhao-Wu Tian[a] and Dongping Zhan*[a]

Received 1st February 2013, Accepted 13th February 2013

DOI: 10.1039/c3fd00008g

The confined etchant layer technique (CELT) has been proved an effective electrochemical microfabrication method since its first publication at *Faraday Discussions* in 1992. Recently, we have developed CELT as an electrochemical mechanical micromachining (ECMM) method by replacing the cutting tool used in conventional mechanical machining with an electrode, which can perform lathing, planing and polishing. Through the coupling between the electrochemically induced chemical etching processes and mechanical motion, ECMM can also obtain a regular surface in one step. Taking advantage of CELT, machining tolerance and surface roughness can reach micro- or nano-meter scale.

Introduction

Electrochemical machining is a non-conventional machining method in which metal materials are removed through anodic stripping or formed through cathodic deposition.[1] The metal workpiece acts as the anode while the tool acts as the cathode, or *vice versa*. Since the tool is guided along the desired path close to but without touching the workpiece, there is no tool wear. Essentially, the kinetic rate of metal electrode processes are very fast and a high metal removal rate is possible without thermal or mechanical stresses. Electrochemical machining can produce high aspect ratio or complex microstructures (*e.g.*, LIGA[2–5] and EFAB[6,7]) and also super-smooth surfaces (*e.g.*, electrochemical mechanical polishing).

However, the workpieces in the above-mentioned electrochemical machining methods must be conductive. Distinct from direct metal processes, the confined etchant layer technique (CELT) is actually an electrochemically induced chemical etching method which is proposed by Prof. Tian in 1992.[8] The principle of CELT is described as follows:[9]

---

[a] *College of Chemistry and Chemical Engineering, and State Key Laboratory for Physical Chemistry of Solid Surfaces, Xiamen University, Xiamen 361005, China. E-mail: dpzhan@xmu.edu.cn; Fax: +865922181906; Tel: +865922185797*

[b] *Center for Precision Engineering, Harbin Institute of Technology, P. O. Box 413, Harbin 150001, China. E-mail: lyhoo@163.com; Fax: +8645186415244; Tel: +8645186412924*

1) Generating the etchant at the surface of the tool electrode:

$$\mathrm{R} \rightarrow \mathrm{O} + \mathrm{ne} \tag{1}$$

Where R is the precursor of etchant and O is the etchant. Actually, the tool electrode used in CELT is both the working electrode and the mold for microfabrication. Due to the diffusion of etchant in the working solution, the shape and thickness are difficult to control. To ensure fabrication tolerance, it is essential to confine the diffusion distance of the etchant in the vicinity of the surface of the tool electrode.

2) Confining the etchant layer to the micro- or nano- meter scale:

$$\mathrm{O} + \mathrm{S} \rightarrow \mathrm{R} + \mathrm{Y} \tag{2}$$

Where S is the scavenger in the working solution, which can react with O and produce R and Y. Due to the scavenging reaction, the etchant is confined at the surface of the tool electrode to form the so-called "confined etchant layer" (CEL). If the concentration of scavenger is significantly higher than the etchant precursor, reaction (2) can be considered as a quasi-first-order reaction. Therefore, the thickness of CEL can be estimated theoretically through the following equation:[9]

$$\mu = (D/K_s)^{1/2} \tag{3}$$

Where μ is the thickness of CEL, D is the diffusion coefficient of etchant in the working solution and K_s is the quasi-first-order reactive rate constant of the scavenging reaction. If K_s were 10^9 s^{-1}, the CEL would be 1 nm.[10] Actually, the thickness of CEL is tuneable experimentally and determines the fabrication tolerance.

3) Microfabrication through chemical etching:

$$\mathrm{O} + \mathrm{M} \rightarrow \mathrm{R} + \mathrm{P} \tag{4}$$

Where, M is the material of the workpiece, which can react with O and produce R and P. When the tool electrode approaches the workpiece and the CEL contacts the surface of workpiece, chemical etching will occur until the microfabrication process is finished.

CELT has been proved successful in the fabrication of 3D microstructures on metals,[11,12] metal alloys[13] and semiconductors.[10,14–17] In general, a molded tool electrode with certain complementary microstructure is used. The mold material can be a Pt–Ir alloy, silicon or PMMA and so on.[10–20] A thin layer of titanium and then a layer of platinum are deposited on the surface of silicon or PMMA layer through magnetron sputtering to make the mold conductive and stable enough as an electrode. For the metal and metal alloy workpieces, protons are generated as the etchant while sodium hydroxide is used as the scavenger. 3D microstructures have been fabricated on copper,[11,21] nickel,[11,22] aluminum,[12] titanium,[23] nitimol,[13] Ti_6Al_4V[23] and Mg alloys.[24] For semiconductor workpieces such as silicon and GaAs, the most commonly used etchant is bromine while L-cystine as the scavenger. Recently, we developed CELT as a polishing method to produce super-smooth surface.[25]

Here we present our recent progress, termed electrochemical mechanical machining (ECMM), in which CELT combines well with the motion modes of conventional mechanical machining. The mechanical cutter is replaced by a tool electrode used in CELT. Thus, mechanical machining operations such as lathing, planing and polishing can be performed by electrochemistry. On one hand, the machining precision is improved by employing the chemical principle of CELT. On the other, the mechanical motions enhance the mass transport and balance of the CELT system. Consequently, the machining efficiency is improved.

Experimental

Chemicals and materials

All chemicals (NaBr, H_2SO_4 and L-cystine) were analytical grade or better and provided by Sinopharm Co., China. GaAs wafer was provided by China Crystal Technologies Co. Ltd, China. All aqueous solutions were prepared with deionized water (18.2 MΩ, Milli-Q, Millipore Co.). Both the cylinder and the linear platinum cutters are prepared through precision machining by our multidisciplinary group. The surface roughness of the cutters is lower than 12 nm and sufficient to be employed as the tool electrode for ECMM.

Instrument

The lab-made ECMM equipment has been described elsewhere previously.[26,27] As shown in Fig. 1, the equipment is composed of four parts: a mechanical motion system, an electrochemical system, a monitoring system and an information-processing computer. In the mechanical motion system, a macro–micro dual driven positioning stage (stepper Z1 and piezo motor Z2) moves the tool electrode accurately in the vertical direction. The workpiece is fixed on the working stage,

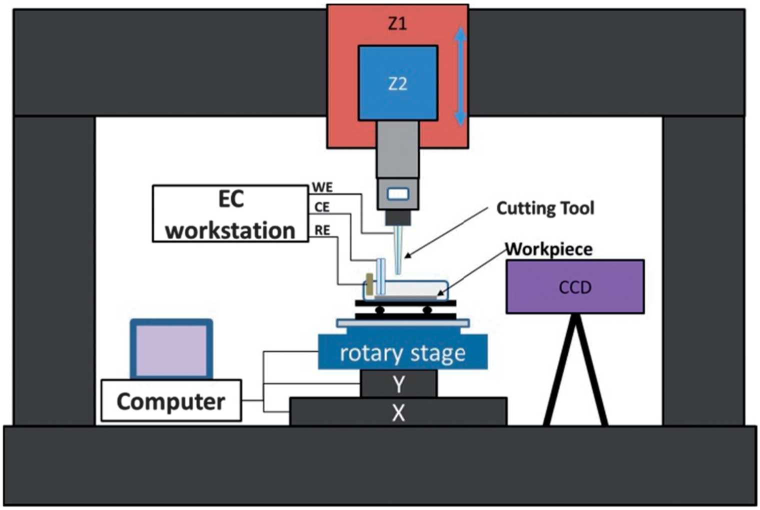

Fig. 1 The schematic diagram of the electrochemical machining instrument, which is composed of a mechanical motion system, an electrochemical system, a monitoring system and an information-processing computer.

which is combined by stepper X, stepper Y and an air-bearing rotary stage (ABRS-150MP-M-X50, Aerotech. Inc., USA). The relative motion between the tool electrode and the workpiece can be programmed in advance. Thus, with the mechanical motion system, almost all mechanical machining processes can be realized. A CHI760 electrochemical workstation (CHI Instrument Co., USA) is used to perform the confined etching processes, including controlling the potential of the tool electrode and detecting the current feedback of the CELT system. The monitoring system includes a force-displacement sensing module and CCD video monitor, which is employed to align the tool electrode with the workpiece, and to control the distance between the tool electrode and the workpiece.[26] Before machining, the working stage is levelled through a SECM current feedback mode as reported previously.[27] Then, the tool electrode is moved to the workpiece by the macro–micro dual driven positioning stage Z with the aid of the CCD video monitor. When the tool electrode touches the workpiece, the force feedback of the force-displacement sensing module changes abruptly, which indicating the zero point of ECMM. After that, the tool electrode is withdrawn for a certain distance, which depends on the expected machining precision. During ECMM, the tool electrode keeps still while the workpiece moves in parallel, vertical or combined manner.

Results and discussion

In the experiments, GaAs wafer was adopted as the workpiece. Considering the mass balance of the ECMM processes, the chemical reactions based on the CELT principle can be formulated as followed:[28]

$$16Br^- \rightarrow 8Br_2 + 16e \tag{5}$$

$$5Br_2 + RSSR + 6H_2O \rightarrow 2RSO_3H + 10Br^- + 10H^+ \tag{6}$$

$$3Br_2 + GaAs + 3H_2O \rightarrow 6Br^- + AsO_3^{3-} + Ga^{3+} + 6H^+ \tag{7}$$

Bromide (Br^-) is used as the precursor to generate the etchant bromine (Br_2) through the electrochemical reaction on the Pt tool electrode. The applied potential is 1.0 V *vs.* SCE. L-Cystine (RSSR) is employed as the scavenger which can react with Br_2. Through the subsequent homogenous chemical reaction, a CEL is formed on the surface of tool electrode. When the CEL contacts the GaAs workpiece, an heterogeneous etching reaction occurs. Actually, the precision is determined by the reaction properties of the chemical etching system but also the concentration ratio of Br^- over RSSR. The confined etching effect of this system is well investigated before and will not be discussed here.[11,16,28]

The first machining process of ECMM is lathing. The tool electrode (or, machining cutter) used in the experiment is a cylindrical Pt electrode with a diameter of 300 μm. As shown in Fig. 2a, a linear pattern on the GaAs workpiece was produced through ECMM. Fig. 2b shows the lateral profile of the obtained pattern. The average width of the grooves is 322.3 μm and the resulting machining tolerance is about 22.3 μm, which shows the good confining effect of CELT. Beside the parallel motion, the workpiece can also rotate. Fig. 3 gives another lathing example in the case of a rotating workpiece, in which a group of

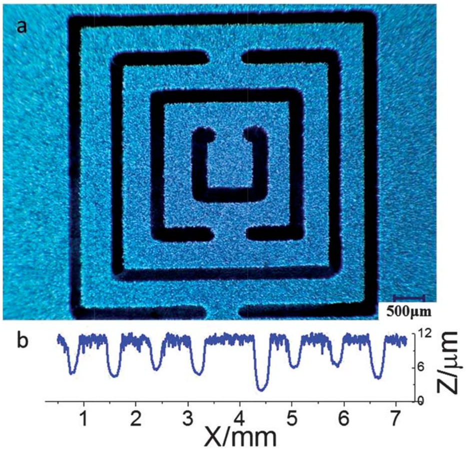

Fig. 2 (a) Optical image of the lathing pattern; (b) profilometric result of lathing pattern in the lateral direction. The working electrolyte solution is an aqueous solution containing 0.3 M NaBr + 0.1 M L-cystine + 2 M H_2SO_4. The distance between the Pt tool electrode and the GaAs workpiece is 25 μm. The moving speed of Pt tool electrode is 60 μm s^{-1}.

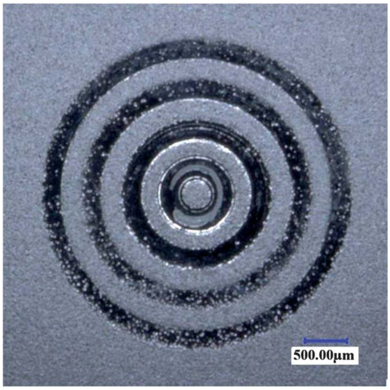

Fig. 3 Optical image of the lathing pattern on a rotating GaAs workpiece. The rotating speed is 2.09 rad min^{-1}; the distance between the GaAs workpiece and the Pt cutting tool electrode is 25 μm.

concentric circles were made through an electrochemical "cutting" process. It should be noted that the product of both the scavenging reaction (6) and the chemical etching traction (7) is bromide, which forms a recycling of Br^-/Br_2 in the narrow space between the tool electrode and the GaAs workpiece. Furthermore, the relative motion between the tool electrode and the GaAs workpiece enhances the mass transport and the balance of the reactant of the CELT system. Thus, the ECMM efficiency and quality can be promoted by optimizing the technical parameters.

ECMM can also be employed to perform planing and polishing processes. Fig. 4 shows the planing effect when the workpiece is moving laterally under a Pt cutting tool electrode with a linear blade shape. The linear platinum blade is 5 mm long, 0.5 mm high and 0.5 mm wide. The moving distance of the Pt cutting

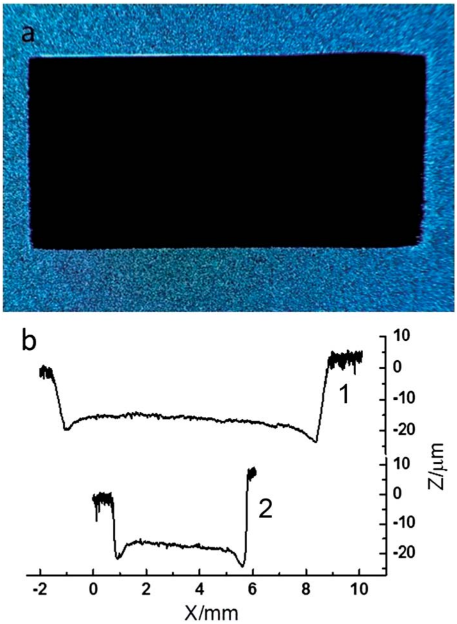

Fig. 4 (a) Optical image of the planing area on a GaAs workpiece; (b) profilometric results of the planing area in the *X* (Curve 1) and *Y* (Curve 2) directions. The working electrolyte solution is an aqueous solution containing 0.1 M NaBr + 0.1 M L-cystine + 2 M H_2SO_4. The distance between the Pt tool electrode and the GaAs workpiece is 25 μm. The moving speed of the Pt tool electrode is 60 μm s^{-1}.

tool electrode is 10 mm. The planing depth is about 16.23 μm while the surface roughness of the planing area is 23.01 nm. From these technological parameters it can be concluded that CELT has a competitive potential to be a planing and polishing method for large-scale supersmooth surface machining.

In general, conventional mechanical machining is a point-by-point cutting operation. However, ECMM provides a possibility to work in a more intensified way. This means that an irregular surface can be formed in one step, resulting in a higher machining efficiency. Fig. 5a shows a case where the GaAs workpiece rotates under a platinum tool electrode with a linear blade shape. The etching depth is bigger in the central area but smaller in the outer area due to the difference of radial-linear velocity. An edge effect can also be observed. This irregular surface is formed through the coupling effect of the CELT etching system and the mechanical motion.

If the chemical etching system of CELT is in steady-state during the ECMM process, as in the case of Fig. 5, a simplified relationship can be derived based on Faraday's law and the mass balance of the CELT system:

$$\int_0^l v\frac{\rho\cdot h\cdot 2\pi\cdot R\mathrm{d}R}{M}=\int_0^l \eta\frac{i\cdot a\cdot \mathrm{d}R\cdot t}{nF} \qquad (8)$$

Where v is the stoichiometric ratio of the etching reaction (7), ρ the density of GaAs, h the etching depth, R the radical distance from the central point, M the molecular weight of GaAs, η the current efficiency, a the width of the tool

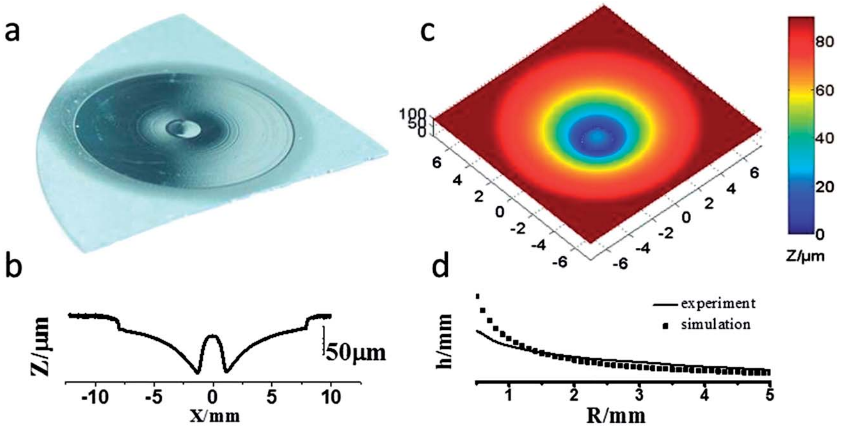

Fig. 5 (a) Optical image of an irregular surface obtained on a GaAs workpiece through the coupling effect of the CELT etching system and the mechanical motion; the rotating speed is 2.09 rad min^{-1} and the distance between the Pt tool electrode and the GaAs workpiece is 10 μm; (b) profilometric results of the irregular surface; (c) a preliminary 3D simulation image of the obtained irregular surface; (d) simulation result of the lateral profile of the irregular surface.

electrode and t the etching time. From eqn (8), the following relationship between etching depth and radical distance can be derived:

$$h = \frac{\eta i a t M}{\upsilon \rho \pi n F} \cdot \frac{1}{R} \quad (9)$$

The preliminary simulation results are shown in Fig. 5c and 5d, which indicates the etching depth is in proportion to $1/R$.

The above examples show the capacity of ECCM to perform large-scale machining with micro- or nano-precision. The last case will show how low in dimensions ECMM can reach. As shown in Fig. 6, the gap between the two grooves (width: 200 μm) is decreased deliberately down to about 10 μm. Then, silver is

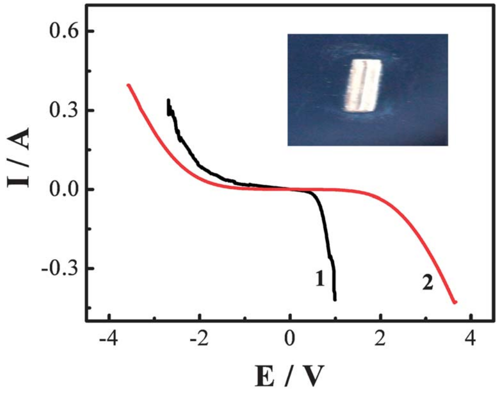

Fig. 6 The *I*–*V* behaviours of the diodes fabricated by ECMM with different gaps: Curve 1 (500 μm) and Curve 2 (10 μm). The insert is the optic microscopic image of the diode with a gap of 10 μm.

electrolessly deposited into the grooves to construct a diode. Curve 2 shows the *I–V* behaviour of this micro-diode. The threshold potential region is doubled that of the comparative macro-diode with a GaAs gap of 500 μm. However, the results seem to show that it might be possible to make simple structures with a size of a micrometer or even nanometers. At present, the fabrication of complex or continuous 3D nanostructures by ECMM remains a challenge.

Since CELT is an *in situ* electrochemically-induced chemical etching process, ECMM can work on conductive, semiconductive and even insulating materials. It can also work on flexible, fragile or fissile materials, even materials harder than the tool. This depends on whether the etching reaction can occur or not, and how fast the etching reaction occurs. Since the tool electrode doesn't contact directly with the workpiece, there is no tool wear and no residual stress the on workpiece. Once the coupling between the chemical process and mechanical motion is optimized, ECMM is highly efficient for both regular and irregular surface machining. In brief, ECMM is a prospective multi-scale machining method with micro & nano precision.

Conclusions

The confined etchant layer technique (CELT) has been developed as a large-scale electrochemical mechanical micromachining (ECMM) method with micro & nano precision. Through the coupling of confined chemical etching and mechanical motion, ECCM can perform conventional lathing, planing and polishing in an electrochemical way. Compared with traditional mechanical machining, ECMM is free of tool-wear, thermal and mechanical stresses due to its confined chemical etching characteristics. Thus, ECMM has prospective applications in micro and nano manufacture.

Acknowledgements

The financial support by the National Science Foundation of China (No. 91023006), the Natural Science Foundation of Fujian Province of China (No. 2012J06004), the National Science Foundation of China (No. 91023047, 91023043, 21061120456 and 21021002), the Fundamental Research Funds for the Central Universities (No. 2010121022), and the Scientific Research Foundation for the Returned Overseas Chinese Scholars (State Education Ministry) are appreciated. Y. Yuan and L. Han have made an equal contribution to this paper. The authors declare no competing financial interest.

Notes and references

1 J. A. McGeough, J. McGeough and J. McGeough, *Principles of Electrochemical Machining*, Chapman and Hall, London, UK, 1974.
2 E. Becker, W. Ehrfeld, P. Hagmann, A. Maner and D. Münchmeyer, *Microelectron. Eng.*, 1986, **4**, 35–56.
3 L. T. Romankiw, *Electrochim. Acta*, 1997, **42**, 2985–3005.
4 Y. Yang, B. Imasogie, S. Allameh, B. Boyce, K. Lian, J. Lou and W. Soboyejo, *Mater. Sci. Eng., A*, 2007, **444**, 39–50.
5 L. Singleton, *J. Photopolym. Sci. Technol.*, 2003, **16**, 413–421.
6 A. Cohen, G. Zhang, F. G. Tseng, F. Mansfield, U. Frodis and P. Will, *EFAB: Batch Production of Functional, Fully-Dense Metal Parts with Micron-Scale Features*, The University of Texas at Austin, 1998.

7 S. E. Alper, I. E. Ocak and T. Akin, *J. Microelectromech. Syst.*, 2007, **16**, 1025–1035.
8 Z. Tian, Z. Fen, Z. Tian, X. Zhuo, J. Mu, C. Li, H. Lin, B. Ren, Z. Xie and W. Hu, *Faraday Discuss.*, 1992, **94**, 37–44.
9 A. J. Bard and L. R. Faulkner, *Electrochemical Methods: Fundamentals and Applications*, Wiley India Pvt. Ltd, 2001.
10 J. J. Sun, H. G. Huang, Z. Q. Tian, L. Xie, J. Luo, X. Y. Ye, Z. Y. Zhou, S. H. Xia and Z. W. Tian, *Electrochim. Acta*, 2001, **47**, 95–101.
11 L. M. Jiang, Z. F. Liu, J. Tang, L. Zhang, K. Shi, Z. Q. Tian, P. K. Liu, L. N. Sun and Z. W. Tian, *J. Electroanal. Chem.*, 2005, **581**, 153–158.
12 L. M. Jiang, X. M. Huang, Z. Q. Tian and Z. W. Tian, *Chem. J. Chin. Univ.*, 2006, **8**, 1540–1544.
13 X.-Z. Ma, L. Zhang, G.-H. Cao, Y. Lin and J. Tang, *Electrochim. Acta*, 2007, **52**, 4191–4196.
14 Y. B. Zu, L. Xie, B. W. Mao, J. Q. Mu, Z. X. Xie and Z. W. Tian, *Electrochemistry*, 1997, **3**, 11–14.
15 Y. Zu, L. Xie, B. Mao and Z. Tian, *Electrochim. Acta*, 1998, **43**, 1683–1690.
16 L. Zhang, X. Ma, J. Tang, D. Qu, Q. Ding and L. Sun, *Electrochim. Acta*, 2006, **52**, 630–635.
17 T. Jing, W. Wen-Hua, Z. Jin-Liang and C. Chen, *Acta Phys.- Chim. Sinica*, 2009, **25**, 1671–1677.
18 L. Xie, J. Luo, B. W. Mao and Z. W. Tian, *Chin. J. Sci. Instrum.*, 1996, **17**, 193–198.
19 Y. Zu, L. Xie, B. Mao and Z. Tian, *Electrochim. Acta*, 1998, **43**, 1683–1690.
20 T. Jing, Z. Li, L. M. Jiang, X. Lei, Y. B. Zu and Z. W. Tian, *Three-Dimensional Electrochemical Micromachining on Metal and Semiconductor by Confined Etchant Layer Technique (CELT)*, 2007.
21 Z. F. Liu, L. M. Jiang, J. Tang, P. K. Liu, L. N. Sun, Z. Q. Tian and Z. W. Tian, *Chin. J. Appl. Chem.*, 2004, **21**, 227–230.
22 Z. F. Liu, L. M. Jiang, J. Tang, L. Zhang, Z. Q. Tian, Z. W. Tian, P. K. Liu and L. M. Sun, *Electrochemistry*, 2004, **4**, 249–253.
23 L. Jiang, W. Li, A. Attia, Z. Cheng, J. Tang and Z. Tian, *J. Appl. Electrochem.*, 2008, **38**, 785–791.
24 L. M. Jiang, Z. Y. Cheng, N. Du, W. Li, Z. Q. Tian and Z. W. Tian, *Acta Phys.- Chim. Sinica*, 2008, **24**, 1307–1312.
25 *CN Pat.*, 201010219037.5, 2010.
26 L. J. Lai, H. Zhou, Y. J. Du, J. Zhang, J. C. Jia, L. M. Jiang, L. M. Zhu, Z. W. Tian, Z. Q. Tian and D. P. Zhan, *Electrochem. Commun.*, 2013, **28**, 135–138.
27 L. Han, Y. Yuan, J. Zhang, X. Zhao, Y. Cao, Z. Hu, Y. Yan, S. Dong, Z.-Q. Tian, Z.-W. Tian and D. Zhan, *Anal. Chem.*, 2013, **85**, 1322–1326.
28 L. Zhang, X. Z. Ma, J. L. Zhuang, C. K. Qiu, C. L. Du, J. Tang and Z. W. Tian, *Adv. Mater.*, 2007, **19**, 3912–3918.